Gating Characteristics of a Steeply Voltage-dependent Gap Junction Channel in Rat Schwann Cells

M. CHANSON,* K.J. CHANDROSS,‡ M.B. ROOK,* J.A. KESSLER,‡ and D.C. SPRAY*§

From the *Departments of Neuroscience, ‡Neurology, and § Medicine, Albert Einstein College of Medicine, Bronx, New York 10461

ABSTRACT The gating properties of macroscopic and microscopic gap junctional currents were compared by applying the dual whole cell patch clamp technique to pairs of neonatal rat Schwann cells. In response to transjunctional voltage pulses (V_j), macroscopic gap junctional currents decayed exponentially with time constants ranging from <1 to <10 s before reaching steady-state levels. The relationship between normalized steady-state junctional conductance (G_{ss}) and (V_j) was well described by a Boltzmann relationship with e-fold decay per 10.4 mV, representing an equivalent gating charge of 2.4. At $V_j > 60$ mV, G_{ss} was virtually zero, a property that is unique among the gap junctions characterized to date. Determination of opening and closing rate constants for this process indicated that the voltage dependence of macroscopic conductance was governed predominantly by the closing rate constant. In 78% of the experiments, a single population of unitary junctional currents was detected corresponding to an unitary channel conductance of ~40 pS. The presence of only a limited number of junctional channels with identical unitary conductances made it possible to analyze their kinetics at the single channel level. Gating at the single channel level was further studied using a stochastic model to determine the open probability (P_o) of individual channels in a multiple channel preparation. P_o decreased with increasing V_j following a Boltzmann relationship similar to that describing the macroscopic G_{ss} voltage dependence. These results indicate that, for V_j of a single polarity, the gating of the 40 pS gap junction channels expressed by Schwann cells can be described by a first order kinetic model of channel transitions between open and closed states.

INTRODUCTION

Gap junction proteins (connexins) are encoded by a multigene family (Beyer, Paul, and Goodenough, 1990; Fishman, Eddy, Shows, Rosenthal, and Leinwand, 1991*a*; Willecke, Heynkes, Dahl, Stutenkemper, Hennemann, Jungbluth, Suchyna, and Nicholson, 1991; Haefliger, Bruzzone, Jenkins, Gilbert, Copeland and Paul, 1992; White, Bruzzone, Goodenough, and Paul, 1992). The juxtaposition of two hemichan-

Address correspondence to Dr. David C. Spray, Dept. of Neuroscience, Albert Einstein College of Medicine, 1300 Morris Park Ave. Bronx, New York 10461.

J. GEN. PHYSIOL. © The Rockefeller University Press · 0022-1295/93/11/0925/22 $2.00
Volume 102 November 1993 925–946

nels (each composed of six connexins), each one of which is located within the membrane of contacting cells, forms channels which provide a pathway for direct metabolic and ionic intercellular communication, or cell coupling (e.g., Bennett and Spray, 1985; Hertzberg and Johnson, 1988; Hall, Zampighi, and Davis, 1993). Gap junctional coupling has been postulated to play important roles in various cell functions, including proliferation (Loewenstein, 1979), differentiation (Warner, Guthrie, and Gilula, 1984), electrical synchronization of contractile cells in heart and vasculature (e.g., Spray and Burt, 1990) and secretion in exocrine and endocrine glands (Meda, Bosco, Giordano, and Chanson, 1991). The diversity of connexins (Cx) expressed by various tissues suggests that the cell-specific distribution of gap junction types may be a determinant factor for tissue function. In agreement with this view, biophysical properties and modulatory mechanisms of gap junctions in different cell types vary, and many of these differences are correlated with the connexin types that form their channels (e.g., Dermietzel, Hwang, and Spray, 1990).

Although a functional role is yet to be demonstrated, gap junction channels close when a difference of potential is achieved between two electrically coupled cells. This type of transjunctional voltage dependence has been reported in invertebrates (Spray, White, Verselis, and Bennett, 1985; Giaume, Kado, and Korn, 1987; Verselis, Bennett, and Bargiello, 1991) and in vertebrate embryonic cells (Spray et al., 1985; Veenstra, 1990). Mammalian gap junctions expressed endogenously were formerly believed to be insensitive to voltage, but voltage dependence of native gap junction channel types has recently been detected between cardiocytes (Rook, Jongsma, and van Ginneken, 1988; Anumonwo, Wang, Trabka-Janik, Dunham, Veenstra, Delmar, and Jalife, 1992; Lal and Arnsdorf, 1992; Wang, Li, Lemanski, and Veenstra, 1992), neonatal astrocytes (Giaume, Fromaget, El Aoumari, Cordier, Glowinsky, and Gros, 1991), adult hepatocytes (Moreno, Campos de Carvalho, Verselis, Eghbali, and Spray, 1991*a*) and adult smooth muscle cells (Moreno, Campos de Carvalho, Christ, Melman, and Spray, 1993). Although most of these tissues express more than one connexin, making it difficult to assign voltage dependent gating to a particular gap junction channel type, exogenous expression systems have begun to address this issue (Dahl, Miller, Paul, Voellmy, and Werner, 1987; Eghbali, Kessler, and Spray, 1990). In these expression systems, mammalian heart-type (Cx43), liver-type (Cx32 and Cx26) and the recently cloned Cx37, Cx42, Cx45 and Cx50 gap junction channels close with increasing transjunctional voltage but with different sensitivities and kinetic properties (Fishman, Moreno, Spray, and Leinwand, 1991*b;* Moreno, Eghbali, and Spray, 1991*b;* Willecke et al., 1991; Barrio, Suchyna, Bargiello, Xu, Roginsky, Bennett, and Nicholson, 1991; Rubin, Verselis, Bennett, and Bargiello, 1992; Veenstra, Wang, Westphale, and Beyer, 1992; White, Bruzzone, Goodenough, and Paul, 1992). Voltage dependence of macroscopic junctional conductance has been quantitatively analyzed in a few systems (Harris, Spray, and Bennett, 1981; Spray, Harris, and Bennett, 1981; Veenstra, 1990; Moreno, Eghbali, and Spray, 1991*b;* Rubin et al., 1992; Wang et al., 1992), but the number of channels present is generally too high to allow steady-state kinetic analysis of the underlying single channel events.

In this study, we have attempted to evaluate both macroscopic and single channel properties of gap junction channels in a novel cell type, neonatal rat Schwann cells in

primary culture. In this system, we found that junctional conductance, measured by applying the dual whole cell patch clamp technique to pairs of cells, was markedly voltage dependent and was low enough to allow resolution of single gap junction channel activity under equilibrium conditions without the use of uncoupling agents. 78% of the cell pairs expressed a single population of gap junction channels with novel properties. The microscopic kinetic analysis of gap junction channel activity in these pairs indicated that the gating of macroscopic junctional conductance by transjunctional voltage could be described by a decrease of the open probability of channels transiting from an open state to a closed state. The possibility of more complex gating mechanisms is also discussed.

MATERIALS AND METHODS

Cell Culture

Schwann cells were obtained from 3–4-d old neonatal rats under asceptic conditions. For each preparation, 30 sciatic nerves were dissected and minced after removal of the perineurium, adjacent connective tissue and blood vessels. Nerve fragments were treated three times for 15 min each at 37°C in calcium- and magnesium-free physiologic saline with glucose containing 0.25% trypsin (GIBCO-BRL, Gaithersburg, MD) and 0.03% collagenase (GIBCO-BRL). The preparation was centrifuged at 700 g for 3 min and the pellet was resuspended and dispersed by trituration using a Pasteur pipette in Dulbecco's Modified Eagle's Medium (DMEM). The resulting suspension was passed through a 60 μm nitex filter and centrifuged at 700 *g* for 5 min. The pellet was resuspended in DMEM supplemented with 2 mM L-glutamine (Sigma Chemical Co., St. Louis, MO), 100 U/ml penicillin, 50 μg/ml streptomycin and 10% heat inactivated calf serum (DMEM-CS) and plated onto a 60-mm diam tissue culture dish pretreated with 10 mg/ml poly-D-lysine (Sigma Chemical Co.). Cultures were maintained at 37°C in a humidified atmosphere of 5% CO_2/95% O_2. On day three after plating, the growth of actively proliferating fibroblasts was arrested by exposing the cultures to 10 μM cytosine arabinoside (Ara-C, Sigma Chemical Co.) in fresh media for 48 h. On day five, the Ara-C was removed and cultures were reared on 60 mm plastic dishes with DMEM-CS containing 10 μl/ml (wt/vol) bovine pituitary extract (Sigma Chemical Co.) and 2 μM forskolin (Calbiochem Corp., La Jolla, CA) in order to stimulate cell proliferation (Brockes, Fields, and Raff, 1979; Porter, Clark, Glaser, and Bunge, 1986). Cells were passaged when confluent monolayers were obtained. Schwann cell purity was determined on the basis of morphology and by using indirect immunofluorescent staining with the primary mouse anti-rat monoclonal antibody 217C directed against the low affinity Nerve Growth Factor receptor which is normally expressed by cultured Schwann cells (generous gift from Drs. J. deVillis [UCLA] and K. Fields [NIH]) used at a dilution of 1:50, and rhodamine-conjugated goat anti-mouse secondary antibodies (dilution of 1:100). Cultures used for studies were 99% pure.

For electrophysiological experiments, confluent dishes were washed several times to remove any residual bovine pituitary extract/forskolin and maintained in DMEM-CS for one week.[1] Cells were then passaged and plated at low density onto glass coverslips pretreated with poly-D-lysine. Electrophysiological recordings made between 1 h and 3 d after plating showed

[1] In a different set of experiments, we found that cAMP elevating agents significantly ($p < 0.01$) increased junctional conductance from a mean ± SEM value of 560 ± 110 pS ($n = 19$) before treatment to 1,230 ± 240 pS ($n = 27$). Removal of these agents decreased junctional conductance to a value (700 ± 194 pS, $n = 12$) similar to that measured in the untreated cells (Chandross, Chanson, Spray, & Kessler, 1992).

no detectable changes in electrical properties of the cells. In one series of experiments, Schwann cells obtained 1 d after dissection were also studied. Again, no difference in junctional channel properties was detected in these cells as compared to the longer term cultures.

Electrophysiology

The glass coverslips were fixed into a small chamber installed on the stage of an inverted Nikon microscope (Diaphot TMF) to allow superfusion of the cells with a solution containing (in mM): CsCl 7, $CaCl_2$ 0.1, NaCl 160, Hepes 10, $MgSO_4$ 0.6, pH 7.2. Junctional conductance was measured by applying the dual whole cell patch clamp technique (Neyton and Trautmann, 1985; White et al., 1985) to Schwann cell pairs. Patch electrodes (2.5–7 MΩ) were pulled and heat polished on a P-87 Flaming-Brown puller (Sutter Instruments, Novato, CA) and were filled with a solution containing (in mM): CsCl 135, $CaCl_2$ 0.5, Na_2ATP 2, MgATP 3, Hepes 10, EGTA 10, pH 7.2. Cesium chloride was chosen to replace potassium chloride in these experiments to reduce activity of nonjunctional channels. Current and voltage recordings were acquired with filtering at 1 kHz using two patch clamp amplifiers (Axopatch-1D, Axon Instruments, Inc., Foster City, CA) and were recorded on a four-channel chart recorder (Gould Instruments, Glen Burnie, MD) and stored on video tape using pulse code modulation (VR-100A, Instrutech Corp. Mineola, NY) for off-line data analysis. After the dual whole cell configuration was achieved, both members of a pair were voltage clamped at a common holding potential of 0 mV. To measure macroscopic junctional conductance (g_j), 10 mV pulses of 300 ms duration were alternatively applied to each cell to generate a transjunctional driving force (V_j). This protocol induced a current both in the pulsed cell and in the nonpulsed cell. While the latter current is only junctional (I_j), the current appearing in the pulsed cell is the sum of junctional (I_j) and nonjunctional currents (I_{nj}). Junctional conductance was then calculated by dividing I_j by the amplitude of the V_j-pulse. Pipette series resistance compensation was used for cell pairs where $g_j > 1$ nS. To evaluate dependence of junctional current on transjunctional voltage, one member of a pair was depolarized or hyperpolarized up to 90 mV for various durations. To allow recovery of junctional conductance between pulses, g_j was monitored by applying small and brief V_j pulses, as described above. In poorly coupled cell pairs, gating of single gap junction channels could be detected. Currents flowing through these channels could be discriminated from other membrane channels as step-like changes of opposite polarities but identical amplitudes recorded simultaneously in both current traces. In 78% of the cell pairs ($n = 25$), a single population of channels (40 pS) was detected, whereas in the seven remaining cell pairs we found additional class of channels of 25–28 pS. These cell pairs were not considered for analysis of microscopic junctional currents, but their presence could not be ruled out in macroscopic measurements.

Data Analysis

Data were played back from video-tape on chart paper after electronic filtering at 30–100 Hz for single channel analysis, or transferred to a computer (316SX, Dell) by means of a digitizing (10 k samples/s) computer interface (VR111, Instrutech Corp.) allowing conversion into ASCII files for macroscopic current analysis. Digitized traces were analyzed using Peakfit Software (Jandel Scientific, Corte Madera, CA) which allows exponential curve fitting.

To determine single gap junction channel conductance (γ_j), the amplitudes of single channel current transitions were measured by hand using a digitizing tablet and customized software. The amplitude of these events was then divided by the applied V_j to obtain conductance values. For each cell pair, conductance values were converted into step-amplitude frequency histograms with bin width of 5 pS. Histograms were fit to Gaussian relations to determine the peak value of the single channel conductance distributions.

To ensure that stationary conditions were met, we waited at least three time constants before collecting data for the binomial distribution analysis. In these experiments, duration of recordings ranged from 30 s to 3 min. Histograms were constructed by summing the open channel event durations at each current level (k) and plotting the relative proportion of time spent in each state (P_k). Manivannan, Ramanan, Mathias, and Brink (1992) have proposed that two tests be used to verify that P_k values are consistent with the expectations of a binomial distribution generated by independent identical channels. Neither of these tests requires knowledge of the number (n) of channels in the patch. In the first test, a parameter R, calculated as $R = P_1^2/P_0P_2 = 2\ n/n - 1$, should decrease monotonically from 4 to 2 as n is

TABLE I

Probabilities in Multichannel Records

Cell pair	n	V_j	P_0	R*	P_k†
No.		*mV*			
1	17	15	0.1818	2.00	$P_2 = 0.278$
	17	25	0.1280	4.00	$P_1 = 0.270$
	17	30	0.0806	3.13	$P_2 = 0.290$
	17	60	0.0235	2.74	$P_1 = 0.307$
2	5	20	0.2184	3.50	$P_2 = 0.209$
	5	40	0.0298	—	$P_1 = 0.138$
3	7	20	0.2076	2.60	$P_2 = 0.280$
	7	30	0.1454	2.60	$P_2 = 0.213$
4	6	20	0.1512	2.49	$P_2 = 0.192$
	6	25	0.1200	3.84	$P_1 = 0.423$
	6	50	0.0012	—	$P_1 = 0.007$
5	4	30	0.0100	—	$P_1 = 0.039$
	4	40	0.0015	—	$P_1 = 0.006$
	4	50	0.0028	—	$P_1 = 0.011$
6	6	40	0.0243	2.66	$P_1 = 0.152$
7	8	30	0.1765	3.80	$P_2 = 0.271$
	8	60	0.0067	—	$P_1 = 0.049$
	8	60	0.0158	2.00	$P_1 = 0.114$
8	20	40	0.0792	2.06	$P_2 = 0.307$
9	4	70	0.0034	—	$P_1 = 0.012$
	4	80	0.0070	—	$P_1 = 0.026$
10	10	90	0.0001	—	$P_1 = 0.002$

n is the maximum number of channels simultaneously seen open.
*In some cell pairs, R could not be estimated because of the absence of occupation of the channels at level $k = 2$. †The second most conductive P_k level is given.

varied from 2 to infinite. In the second test, an upper bound for P_k can be calculated for $k > 0$ and not the most conductive level (Manivannan et al., 1992), $P_k = (k/k + 1)^k$. These bounds are $P_1 < 0.5$, $P_2 < 0.44$ and $P_3 < 0.42$. To verify that the data sets used in our calculations satisfied these conditions, these two tests were applied to the P_k distributions (Table I). Of 25 original data sets, three did not satisfy one criterion or the other, and those data were not used for subsequent analysis. Plots of data presented here were generated using software (Sigmaplot, Jandel Scientific) capable of curve-fitting by least squares with any explicit user function.

RESULTS

Macroscopic Currents

Junctional conductance was evaluated in 70 pairs of Schwann cells immediately after establishment of the dual whole-cell configuration and was monitored throughout the recordings which lasted between 10 and 45 min. As shown in Fig. 1, macroscopic junctional conductance (g_j) between Schwann cells was low, averaging 460 ± 65 pS (mean ± SEM). As expected for the low degree of coupling between cell pairs, fluctuation of g_j was often detected during recording.

To evaluate voltage dependence, long transjunctional voltage (V_j) pulses were used. As shown in Fig. 2, junctional currents (labeled I_1) decreased with time to reach steady-state levels for transjunctional voltages >10 mV, the relaxation occurring more rapidly and to a lower steady-state level with increasing driving forces. To determine the sensitivity of g_j to transjunctional voltage, data were analyzed as

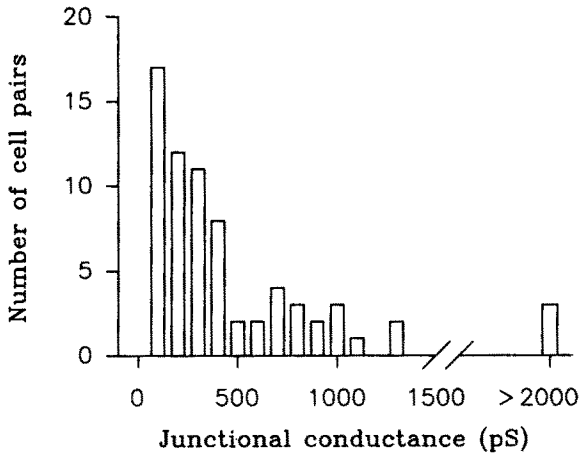

FIGURE 1. Frequency distribution of macroscopic junctional conductances measured between Schwann cell pairs. Conductances measured from 70 experiments were grouped in bins of 100 pS. Junctional conductance between these cell pairs was generally low, being <500 pS in 50% of Schwann cell pairs examined.

illustrated in Fig. 3 (*top*). For each data set, the current-voltage relationship was constructed for the steady-state junctional current (I_{ss}, reached at the end of each voltage pulse) and for the initial junctional current ($I_{(0)}$) measured at the start of each V_j pulse. $I_{(0)}$ was found to be a linear function of V_j within the V_j range ± 60 mV; therefore, the steady-state junctional conductance can be expressed for various V_j's as $G_{ss} = I_{ss}/I_{(0)}$. This procedure provides a convenient method to normalize data from cell pairs with different g_j. The individual G_{ss} data points (*inset*) as well as the averaged values (mean ± SEM) obtained from 19 cell pairs are shown in Fig. 3 (*bottom*). G_{ss} decreased markedly with increasing V_j of either polarity to reach virtually zero at potentials larger than 60 mV. This dependence of g_j on V_j was independent of the absolute membrane potentials of the cells (inside-out voltage dependence). Indeed, simultaneous sustained depolarizations or hyperpolarizations (±30–50 mV) of both members of the cell pairs did not affect junctional conductance as evaluated by superimposing 10 mV pulses of 300 ms duration (not shown).

For channels that transit between one open and one closed state, and where the energy difference between the states is a linear function of voltage, the equilibrium distribution between these two states (the normalized steady-state junctional conductance; G_{ss}) can be described by a Boltzmann relation of the form (Spray et al., 1981):

$$G_{ss} = (G_{max} - G_{min})/\{1 + \exp[A(V_j - V_0)]\} + G_{min}, \quad (1)$$

where G_{max} represents the upper limit of the Boltzmann relation and G_{min} is the residual G_{ss} reached at very large V_j. Because of normalization, G_{max} and G_{min} are dimensionless. V_0 is the value of V_j at which the voltage sensitive portion of steady-state junctional conductance ($G_{max} - G_{min}$) is decreased by 50% and A is a parameter quantifying voltage sensitivity. A is defined as nq/kT where n is the equivalent number of charges of valence q (gating charges) moving through the entire voltage field, and kT has its usual significance.

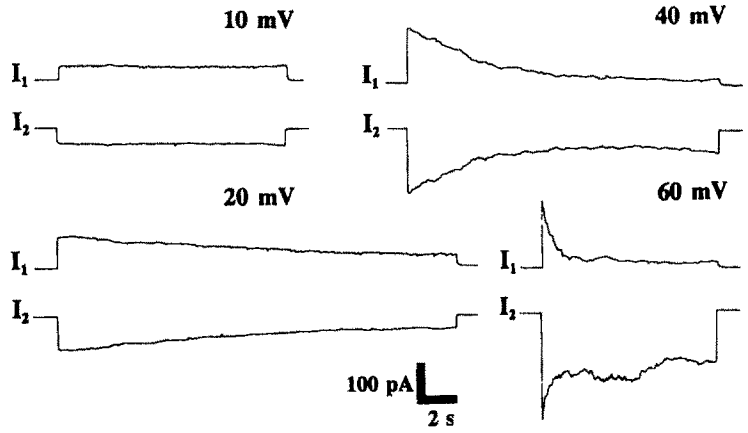

FIGURE 2. Examples of extent and time course of current relaxations elicited by transjunctional voltages of 10, 20, 40, and 60 mV in a Schwann cell pair. When one cell of the pair was hyperpolarized, a junctional current (I_1) could be measured in the other cell. This current declined during the pulse to reach a steady-state level at driving forces >10 mV. The current (I_2) measured in the polarized cell is composed of both junctional (I_1) and nonjunctional currents.

As is illustrated in the lower panel of Fig. 3, the sensitivity to voltage was such that G_{ss} was not equal to G_{max} at V_j close to 0 mV. To obtain the Boltzmann parameters, therefore, G_{max} was left as a free parameter during the fitting procedure. In four distinct cell pairs that were subjected to curve fitting, G_{max} averaged 1.25 ± 0.12 (mean ± SEM, normalized with respect to $G_{ss} = 1$ at $V_j = 0$ mV). For the collated data from 19 cell pairs illustrated in Fig. 3, the best fit of G_{ss} to the Boltzmann relations in both polarities was obtained for $G_{max} = 1.33$, $V_0 = \pm 15$ mV and $A = 0.096$ (*solid line, bottom*). Assuming a valence of 1, this value of A corresponds to an equivalent gating charge n of 2.4, or, expressed another way, to an e-fold decrease in G_{ss} per 10.4 mV. Note that for these cells, steady-state junctional conductance

reached zero at V_j's > 60 mV, demonstrating the absence of any residual G_{ss} component; thus $G_{min} = 0$.

To analyze the kinetics of junctional current relaxations at various V_j's, junctional currents were digitized and the relaxations were fit to exponential functions. As shown in Fig. 4 (*top*, digitized currents corresponding to traces in Fig. 2), the relaxation of the junctional currents (I_j) from their initial levels ($I_{(0)}$) to their steady-state values (I_{ss}) was well fit by a single exponential equation (solid lines drawn

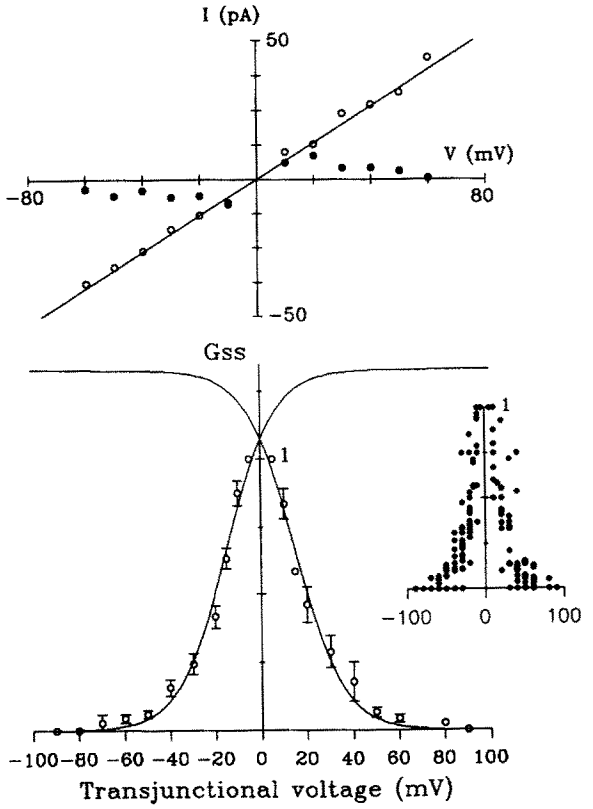

FIGURE 3. Dependence of initial and steady-state junctional currents on transjunctional voltage. (*Top*) $I_j - V_j$ relationship in a Schwann cell pair. For each V_j applied as in Fig. 2, instantaneous ($I_{(0)}$) and steady-state (I_{ss}) junctional currents were measured at the beginning of the command pulse (*open circles*) and at its end (*solid circles*). Within the V_j range studied, the $I_{(0)}$ relation for the representative cell pair illustrated is linear with a slope (determined by linear regression) of 660 pS. By contrast, I_{ss} deviated from linearity for V_j pulses as small as 10 mV. (*Bottom*) The normalized steady-state junctional conductance ($G_{ss} = I_{ss}/I_{(0)}$) at various V_j's was calculated in 19 cell pairs and plotted as mean ± SEM (*open circles*) as a function of transjunctional voltage of both polarities. Individual G_{ss} values in all experiments are illustrated in the inset to provide additional indication of variability. G_{ss} decreased with increasing voltages of either sign after a Boltzmann relation (see text). Best fit (*solid lines*) was obtained for V_0 = ±15 mV, G_{max} = 1.33, and A = 0.096. G_{ss} approached zero at V_j's > 60 mV indicating the absence of a voltage independent component, G_{min}.

through the data) of the form (Harris et al., 1981):

$$I_j = (I_{(0)} - I_{ss})\exp(-t/\tau) + I_{ss} . \quad (2)$$

For the traces illustrated, time constants (τ) of 7.6, 3.34 and 0.49 s were obtained for current relaxations elicited by driving forces of 20, 40, and 60 mV, respectively ($r^2 > 0.9$ in all cases). The current trace corresponding to a driving force of 10 mV was not processed for curve-fitting (see below). Averaged τ determined from several data sets over a wide range of V_j's are illustrated in the upper panel of Fig. 5. The

longest time constants (~8 s) corresponded to V_j's near V_0; τ strongly declined to minimal values with increasing voltages (< 1 s at V_j's > 50 mV). At V_j < 15 mV, a meaningful value for τ could not be determined from long pulses because of the absence of a measurable current decay. For a first order process, however, τ at 10 mV

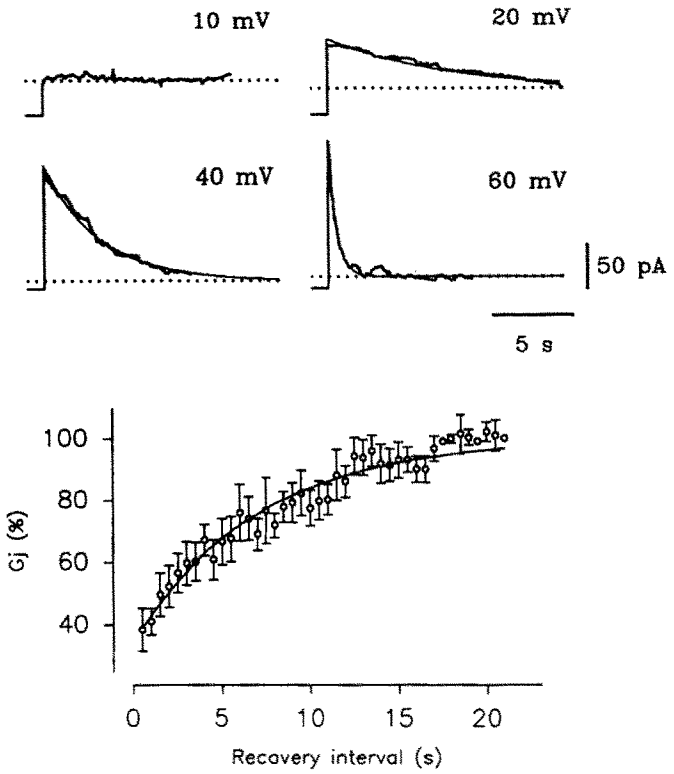

FIGURE 4. Exponential time course of junctional current relaxations. (*Top*) The temporal decays of the junctional currents illustrated in Fig. 2 were processed for exponential curve-fitting from the initial current value to the steady-state current level (*dotted line* in each plot). With the exception of the current induced at 10 mV, data were well fit ($r^2 > 0.9$) by single negative exponentials. Time constants derived from the best fit (*solid line superimposed to the current trace*) decreased markedly with increasing transjunctional voltages with values of 7.6 s at 20 mV, 3.34 s at 40 mV, and 0.49 s at 60 mV. (*Bottom*) The time constant at low driving force was evaluated from the time course of junctional conductance recovery at V_j = 10 mV after a large prepulse (ranging between 30–60 mV). In seven experiments, g_j was measured each 0.5 s by imposing 5–10 mV V_j pulses of 100 ms duration. Values were normalized to the maximal junctional conductance (G_j) reached at the end of the recovery protocol and plotted as mean ± SEM as a function of time (recovery interval). The time course of G_j recovery can be well described by a single exponential curve with a time constant of 7.1 s ($r^2 = 0.95$).

can be obtained from the time course of g_j recovery at this voltage after larger pulses of the same polarity. As is illustrated in Fig. 4 (bottom), data from seven experiments were averaged and processed for exponential curve fitting. Best fit was obtained for a time constant of 7.1 s ($r^2 = 0.95$).

For a first order process $\tau = 1/(\alpha + \beta)$ and $G_{ss} = \alpha/(\alpha + \beta)$, opening ($\alpha$) and closing ($\beta$) rate constants were calculated for all applied driving forces according to the equations:

$$a = G_{ss}/\tau \quad \text{and} \quad \beta = (1 - G_{ss})/\tau\,. \tag{3}$$

Values for α and β calculated from the collated data are represented as a function of transjunctional voltage in Fig. 5 (*bottom*). Substituting in the above equations and

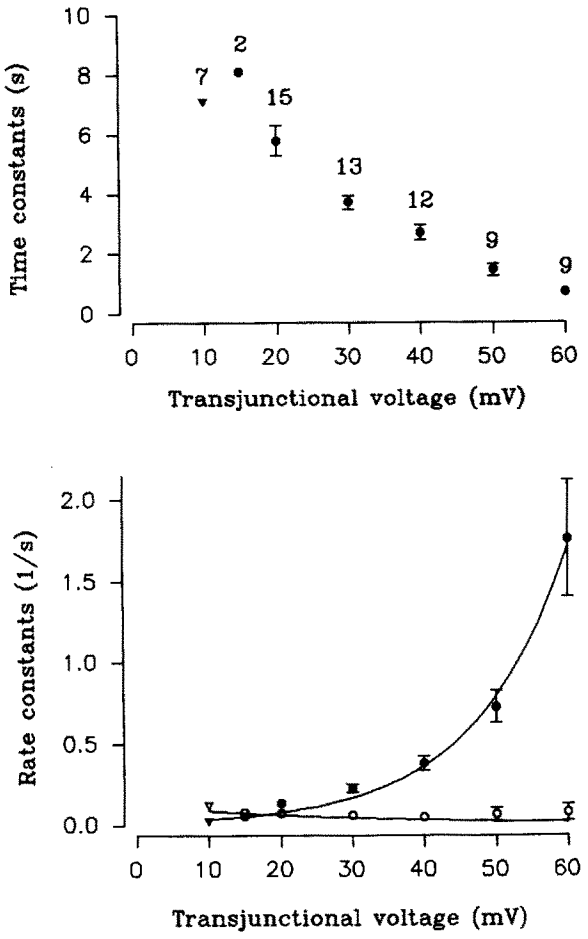

FIGURE 5. Voltage dependence of time and rate constants. (*Top*) Time constants (τ) as determined from best fit of junctional current decays at various V_j's of the number of experiments indicated in the graph were plotted as mean ± SEM versus transjunctional voltage. (*Bottom*) With the exception of values at V_j = 10 mV, α (*open circles*) and β (*filled circles*) were determined for each transjunctional voltage by using the time constant and the steady-state level determined by the fitting procedure, and are plotted as mean ± SEM versus V_j. α and β values at 10 mV (*triangles*) were determined from G_{ss} and τ values as evaluated in the lower panels of Figs. 3 and 4, respectively. The solid lines drawn through α and β are the best fits calculated from the equations given in the text. In contrast to the strong voltage sensitivity of β, α showed weak voltage dependence over the entire V_j range examined.

defining a parameter k (the rate at which $\alpha = \beta$, reached at $V_j = V_0$), the relation between the rate constants and voltage can be described by (Harris et al., 1981):

$$\alpha = k \exp[-A_\alpha(V_j - V_0)] \text{ and } \beta = k \exp[A_\beta(V_j - V_0)]\,, \tag{4}$$

where A_α and A_β are the respective voltage sensitivities of each rate constant. Best fits to experimental data occurred when $k = 0.065$, $A_\alpha = 0.033$, $A_\beta = 0.078$ and $V_0 = 18$ mV. The opening rate constant was weakly voltage dependent; at higher voltages, the

closing rate constant predominated in determining whether the channels were open or closed.

The time course of junctional conductance recovery at V_j = 0 mV was monitored by superposing subthreshold voltage pulses at the termination of a sustained V_j of 40 mV. g_j recovery at 0 mV was well fit by a single exponential with a time constant of 4.7 ± 0.3 s (n = 5, mean ± SEM), which is in reasonable agreement with expectations from extrapolation of τ values in Fig. 5 (*top*) to 0 mV. Together, these observations are consistent with the scheme that the junctional channels undergo first order transitions between conducting (*open*) and nonconducting (*closed*) states.

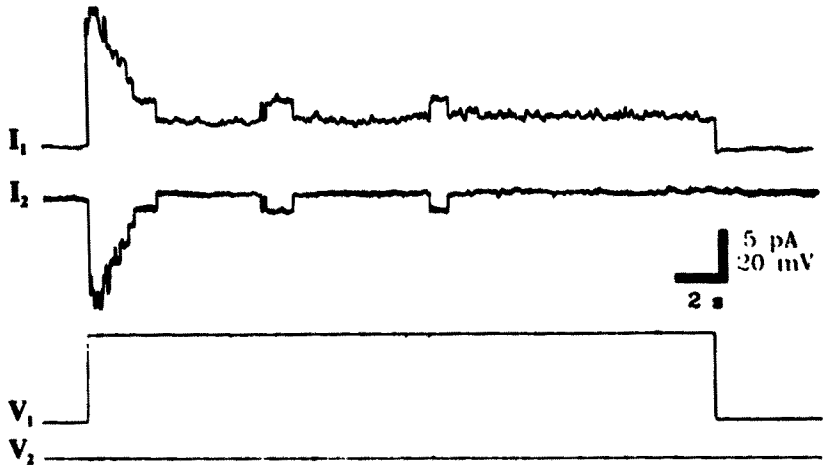

FIGURE 6. Voltage dependence of junctional current relaxation in a weakly coupled Schwann cell pair. At the beginning of the experiment, both members of the cell pair were held at 0 mV. Depolarization of one cell to 40 mV (V_1) elicited currents (I_1 and I_2) in each cell, I_2 being of opposite sign. I_2 represents the junctional current while I_1 is the sum of junctional and nonjunctional currents. The contribution of the nonjunctional component can be evaluated by the residual current in I_1 detected at the end of the pulse. During the transjunctional voltage step, the junctional current decreased in a step-like manner to reach a steady-state level. Single gap junction channel openings and closures are recognized by simultaneous transitions of identical but opposite polarities in both cells of the pair. In this cell pair, the steady-state level of I_2 corresponds to zero junctional conductance, indicating the absence of a voltage-independent junctional conductance. In this recording, I_1 was filtered at 15 Hz and I_2 at 50 Hz.

Microscopic Currents

Fig. 6 illustrates a typical recording from a cell pair in which few channels (in this case, seven) were detected. When a 40 mV driving force was applied, the junctional current (I_2) decreased in a step-like manner to reach a steady-state level of activity within seconds. This activity consisted of opening and then closing of single gap junction channels from a baseline which corresponded to zero open channels (as indicated by the absence of any current deflection at the end of the pulse).

To determine whether the voltage dependence of macroscopic junctional current was caused in part by a change in the unitary conductance (γ_j) of gap junction

channels, single gap junctional channel current transitions were measured at different driving forces. From a total of 2,193 current transitions (25 cell pairs), values obtained for each driving force were averaged and plotted as a function of V_j (Fig. 7). As shown in the top left panel, channel currents increased linearly with voltage, with a slope conductance of 39 pS. Frequency histograms of unitary junctional conductance values determined at 20 mV (*top right*), 40 mV (*lower left*) and 60 mV (*lower right*)

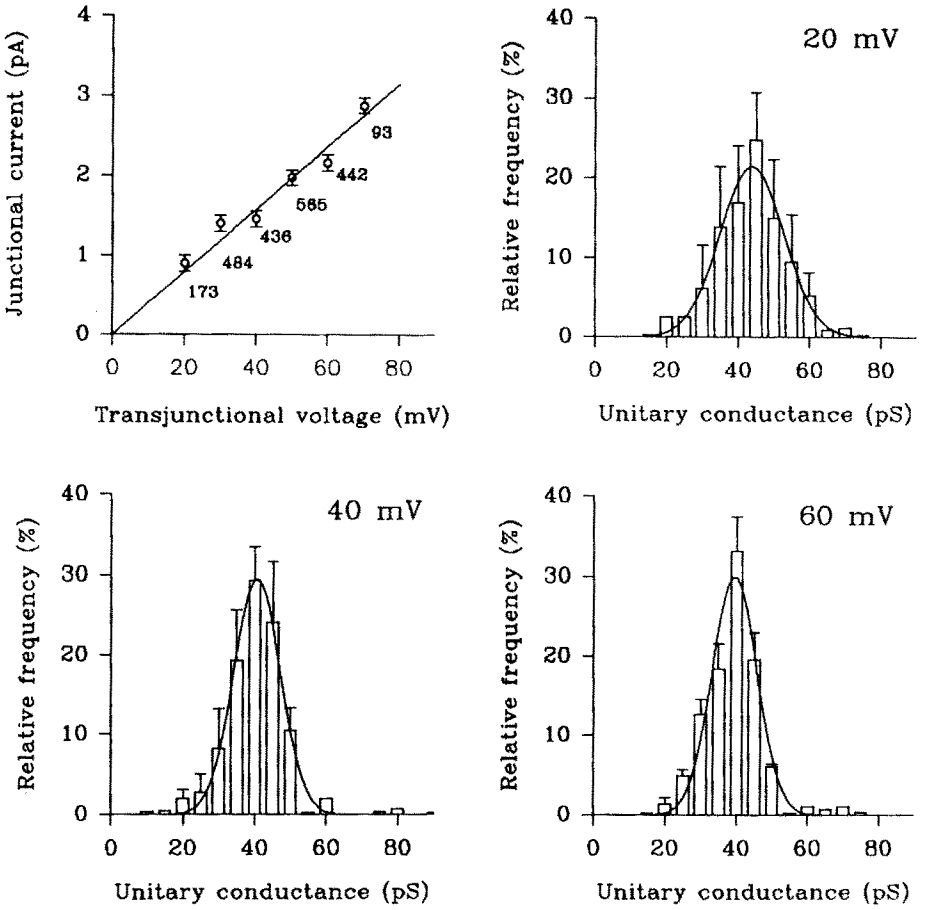

FIGURE 7. Unitary conductance of the gap junction channels expressed by Schwann cells. Currents through individual gap junction channels were measured at different transjunctional voltages and plotted as mean ± SEM of a total of 2,193 current transitions (upper left panel). Values increased linearly with voltage with a slope of 39 pS as determined by linear regression. Frequency histograms of conductance values calculated from all current transitions grouped in bins of 5 pS are also shown for V_j of 20 mV (upper right panel), 40 mV (lower left panel) and 60 mV (lower right panel). The distribution of values was well fit by Gaussian relations (solid line in each plot) with a single peak of 43 pS at 20 mV (n = 173 events, 4 experiments), 41 pS at 40 mV (n = 248 events, 6 experiments) and 39.5 pS at 60 mV (n = 246 events, 3 experiments). This indicates that currents were carried by only one type of channel with voltage-independent unitary conductance.

are also illustrated in Fig. 7. For each V_j, values showed a single distribution which could be described by a Gaussian relation with means ranging between 39 and 44 pS. These observations indicated that the junctional current is carried through a single population of channels having a voltage independent unitary conductance.

To evaluate the dependence of the open probability (P_o) of gap junction channels on transjunctional voltage, we used a statistical approach for multi-channel data analysis. This is based on the binomial distribution of the probability P_k to find k channels open out of n total channels (Colquhoun and Hawkes, 1983):

$$P_k = [n!/k!\,(n-k)!]\,P_o^k\,(1-P_o)^{n-k}, \tag{5}$$

where P_o is the open probability of each of the n channels. This method assumes that all channels are identical and that they are gated independently of one another. Using this equation, P_o can be estimated if n and P_k are known. Because our interest was primarily to assess whether a fit using independent identical channels was consistent with the data recorded, we have not used sophisticated tests to verify our estimates of the number of channels present at the junctional membrane. Instead, n was estimated by counting the number of open channel levels in which I_j was observed to reside before reaching the zero level during a voltage step; although this estimate therefore represents a lower bound on n, our best fits to the P_k values indicated that increasing n did not result in improved description of the data (see below). P_k was determined for each V_j under steady-state conditions by determining the ratio between the time spent by I_j at each of the specific open channel levels and the total recording time.

Results of representative measurements of residence times at each conductance level ($k = 0$ to n) are shown in Fig. 8 (where data are represented by bars in each plot and prediction from the binomial equation by *filled circles*). The top shows the distribution of P_k at $V_j = 25$ mV obtained from a cell pair apparently connected by 17 channels. An example of the single channel activity in this cell pair is shown in the right hand panel. At this driving force, the channels spent most of their time between levels one and three. This behavior was well fit (*filled circles*) by the binomial distribution which predicts a P_o of 0.128 for each channel. When the driving force was increased to 60 mV, single channel activities were restricted to lower levels (example to the right) and the P_k distribution was shifted to the left (Fig. 8, *middle*); the P_o predicted by the binomial fit was reduced to 0.0235 at this voltage. The lower panel of Fig. 8 shows an example of P_k distribution at a driving force of 80 mV in another cell pair, which was apparently coupled through only four junctional channels. At this V_j, the channels almost always remained in the closed state ($P_o = 0.007$), a few brief opening events being detected occasionally (example to the right).

P_o values determined at various V_j in 22 experiments on 10 different cell pairs by applying the binomial distribution are listed in Table I. In all cases, we attempted to improve the best fit by increasing the number of channels; however, these attempts resulted in poorer fits (not shown). The values for R and P_k presented in Table I are consistent with the two tests for independent identical channels.[2] Note from this table

[2] R and P_k terms are derivations from Eqs. 4 and 6 of Manivannan et al., 1992 (see also Materials and Methods). Methods).

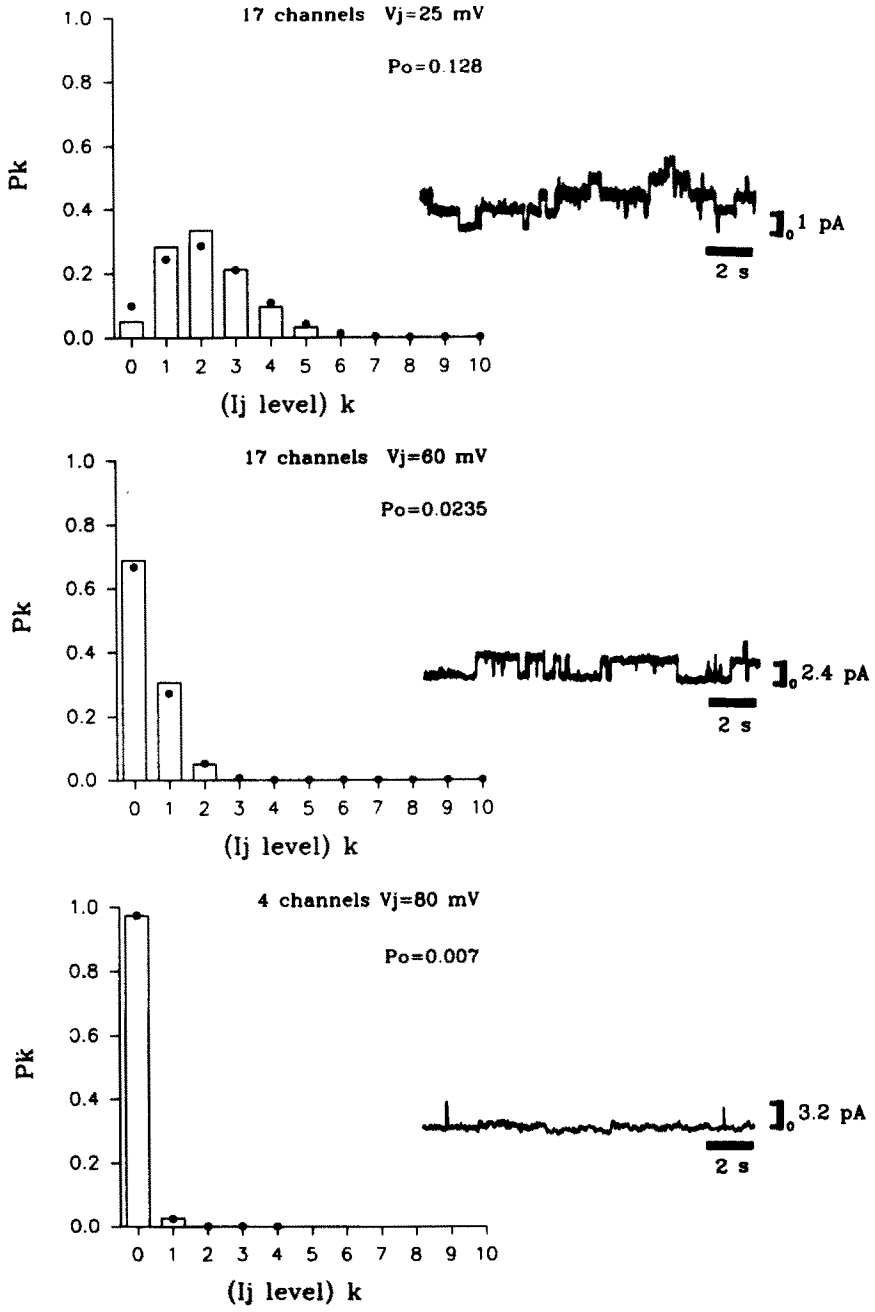

FIGURE 8. Effect of transjunctional voltage on the open probability of gap junction channels. (*Top and middle*) Examples of the distribution of the probability of 0, 1, 2, . . . , k = 17 open gap junction channels (P_k) at transjunctional voltages of 25 (*top*) and 60 mV (*middle*), respectively. At 25 mV driving force, several levels corresponding to particular numbers of open channels were detected in the junctional current trace shown in the right part of the figure (0 at the lower limit

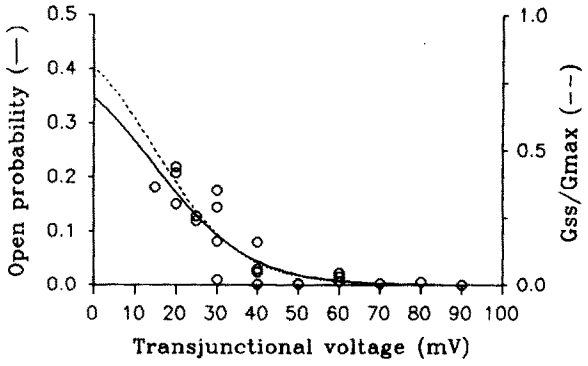

FIGURE 9. Relationship between channel open probability and transjunctional voltage. The open probability of gap junction channels was deduced from binomial distributions applied to single channel activity recorded in 20 experiments on 10 cell pairs monitored at various transjunctional voltages. Duration of experiments ranged from 30 s to 3 min. The decrease of P_o values with increasing voltages followed a Boltzmann relation (*solid line*). This fit is similar in shape to the relation describing voltage dependence of macroscopic currents ($G_{ss} - V_j$ fit) shown in Fig. 3. The latter curve (plotted as a *dashed line*) was normalized to G_{max} and was redrawn after scale adjustment to allow visual comparison with the P_o fit.

that tests were satisfied for individual cell pairs throughout the course of an experiment, even when driving force was changed, indicating that recordings were quite stable. Fig. 9 illustrates the relationship between P_o and V_j obtained from 22 experiments (*open circles*). The distribution of P_o values can be fit by a Boltzmann relation (*solid line*) with $A = 0.0878$ and $V_0 = 15$ mV. This relation is similar in shape to that describing the voltage dependence of macroscopic junctional currents (Fig. 9, where the dashed line is redrawn from Fig. 3), suggesting that the voltage dependence of macroscopic g_j can be attributable to the effect of V_j on P_o. The P_o value at the zero voltage intercept of the solid curve in Fig. 9 is 0.34, indicating that the open probability of gap junction channels in the absence of driving force is much less than unity. Note that the two ordinates in Fig. 9 represent different scales. Although P_o determined by single channel measurements corresponds to the true P_o of the channel, the macroscopic measurements represent only the relative probability of the fraction of open channels showing voltage dependence.

The decrease of the time spent by the channels in the open state with increasing V_j, as illustrated in Fig. 8, suggests that the life time of the channels is also affected. Direct measurements of closed time is difficult in multichannel recording. However,

---

of the scale indicates the zero current level when all channels are closed). Measurement of the time spent by the junctional current at each level of open channels and normalization to the total time of the recording allowed estimation of P_k. The distribution of P_k values (*bars*) expressed as a function of k levels (only 10 out of the 17 levels are represented in the figure) was well fit by the predicted values of a binomial distribution (*filled circles*) with a single channel open probability $P_o = 0.128$. At a driving force of 60 mV, single channel activity was restricted to lower levels, the P_k distribution being well fit by a binomial distribution with a $P_o = 0.0235$. (*Bottom*) Example of single channel activity and P_k distribution of four junctional channels detected in another cell pair. At a transjunctional voltage of 80 mV, the channels remained closed almost all the time, brief openings being only occasionally detected. The open probability determined by the binomial distribution was $P_o = 0.007$. Note from the representative records that the open lifetimes also decreased with higher V_j.

open time of the channels could be determined in some cell pairs by measuring the duration of current transitions from the zero open channel level to the first level of opening, and back again to the baseline. Because of filtering, 50 ms was the minimum duration which we considered in these measurements. Open time durations obtained at various driving forces were pooled from various experiments, and averaged 1,620 ± 39 ms (n = 22) at V_j = 20 mV, 920 ± 15 ms (n = 53) at V_j = 30 mV, 740 ± 4.6 ms (n = 144) at V_j = 50 mV and 360 ± 3.6 ms (n = 49) at V_j = 60 mV. Although these measurements can only be considered to be preliminary estimates of the mean open time because the number of events measured is rather low, these data clearly show that the average time the channels stayed open markedly decreased with increasing V_j.

Previous modeling studies indicated that gap junction channels closed by a V_j of

FIGURE 10. Effect of voltage polarity reversal on activity on a small number of gap junction channels. In this recording, one cell of a pair was hyperpolarized to −40 mV (the *lower trace* illustrates the voltage protocol). This induced a junctional current (*upper trace*) which by discrete channel closures relaxed with time to the zero current level. At steady-state, I_j travelled between the levels of only one or two open channels. At the end of the hyperpolarizing pulse, the potential was reversed to +40 mV. At this time, junctional current increased after a short delay, decreasing thereafter to the zero current level, indicating that gap junction channels transited through the open state before closing again in response to the driving force of opposite polarity. Current was filtered at 100 Hz.

one polarity must reopen before being closed by a voltage of the other polarity (Harris et al., 1981), which would imply that channel openings should be detectable in few channels recording after such a polarity reversal. The behavior of Schwann cell gap junction channels when the transjunctional voltage is switched from a voltage inducing their closure to the reverse polarity was studied in 6 low conductance cell pairs. In the recording illustrated in Fig. 10, a driving force of −40 mV was first applied, leading to the step-like decrease of junctional current until the level of zero conductance was reached. At this steady-state level, the activity of only two channels can be detected. When the V_j polarity was reversed, the closed channels reopened transiently before closing again to reach the minimum level. The latency of the peak junctional current after the polarity was reversed was almost 2 s, which is primarily attributable to the slow rate of channel opening before being closed by V_j.

DISCUSSION

We have studied the biophysical properties of macroscopic and microscopic gap junctional currents in pairs of rat Schwann cells maintained in culture. In addition to describing the properties of a novel gap junction channel, we sought to determine whether several assumptions raised by modeling of macroscopic junctional currents (Harris et al., 1981; Spray et al., 1981) were confirmed at the single channel level. We showed that, for the majority of these cell pairs (78%), junctional current is carried through a single type of identifiable channel and is strongly dependent on transjunctional voltage (V_j). Junctional current relaxation during a V_j step is the result of a voltage dependent decrease of the open probability (P_o) and is not due to a change in the channel's unitary conductance. Although voltage dependent gating of gap junction channels was first described quantitatively more than a decade ago (Harris et al., 1981; Spray et al., 1981), assignment of characteristics to specific connexin types and determination of gating mechanisms have been difficult. Part of the problem has been the preparations which have been used for study. Cells of most tissues generally express more than one type of connexin, and the large number of channels present at most junctional membranes requires the use of gap junction blocking agents (such as long-chain alcohols or halothane) which themselves affect single channel gating properties, including P_o. Compared with the other preparations that have been studied, rat Schwann cells therefore offer a good model for studying the biophysical properties of gap junctions on the single channel level.

Mammalian connexins generally show weak to moderate transjunctional voltage dependence with equivalent gating charges ranging from 1.9 for Cx32 (Moreno et al., 1991*b*) to 3.9 for Cx26 expressed in oocytes (Rubin et al., 1992). Moreover, V_j at which voltage dependence occurs is usually large (V_0 = 25–90 mV) and a residual conductance component (G_{min} = 0.1–0.5) has been detected in all previous studies (Barrio et al., 1991; Fishman et al., 1991*b;* Moreno et al., 1991*b;* Rubin et al., 1992; Veenstra et al., 1992; Willecke et al., 1991). By comparison, Schwann cells showed an intermediate voltage dependence steepness (gating charge = 2.4), but junctional current relaxed completely to zero at large transjunctional voltages (G_{min} = 0) with a half inactivation V_0 = 15–18 mV. Whether the residual voltage insensitive conductance component (G_{min}) observed in other preparations arises from channel subconductance states, saturation of the rate constants or presence of another channel population remains unclear and may vary from one preparation to another.

The relaxation of junctional currents elicited by transjunctional voltages followed a single exponential decay, the gating of the channels being predominantly governed by the closing rate constant while the opening rate constant appeared to be weakly voltage dependent. The limited temporal resolution of whole cell recording in pairs of cells might obscure a very rapid initial gating mechanism. While this possibility cannot be totally ruled out, it is not supported by the single channel data which showed a single population of channels and the absence of substates. In addition to the fact that junctional conductance recovery also followed a single exponential process, these observations argue in favor of a simple model with first order kinetics to describe the gating of gap junction channels expressed in Schwann cells.

The binomial model has been employed recently to determine whether gap

junction channels found in the septal membrane of earthworm behave independently (Manivannan et al., 1992) and to study voltage dependence of homo- and heterologous junctional channels in mixed cultures of neonatal cardiac rat fibroblasts and myocytes (Rook, van Ginneken, de Jonge, El Aoumari, Gros, and Jongsma, 1992). The binomial distribution allows description of the stochastic behavior of identical independent channels (Colquhoun and Hawkes, 1983). In Schwann cells, 78% of the cell pairs studied showed a homogeneous population of junctional channels with unitary conductance that was not affected by transjunctional voltage, a property in common with other gap junction channel types (Neyton and Trautmann, 1985; Veenstra & DeHaan, 1986; Rüdisüli and Weingart, 1989; Veenstra, 1990; Moreno et al., 1991*b*; Rook et al., 1992). The occupancy of discrete conductance levels by I_{ss} (indicating whether 1, 2, . . . , k channels were open at a given time) was well described by a binomial distribution at all the transjunctional voltages studied, suggesting that Schwann cell gap junction channels behave independently of each other. This situation is in agreement with the original proposal by Harris et al. (1981), but may not be generalizable to gap junctions in all tissues (Manivannan et al., 1992). With increasing transjunctional voltage, the open channel distribution shifted to the lower levels because of a reduction of the open probability. The relationship between P_o and V_j can be described by a Boltzmann function of the same shape as that describing voltage sensitivity of macroscopic junctional currents. These observations indicate that the voltage dependent decrease in macroscopic junctional conductance can be ascribed to the decrease of the open probability of the channels, and support the two-state (*open and closed*) model deduced from time courses of macroscopic current relaxations.

Boltzmann modeling of steady-state junctional conductance and estimation from rate constants of the fraction of open channels both differed from unity in the absence of a potential difference across the junctional membrane. Whereas these data indicate that gap junction channels in this system are continually opening and closing at V_j = 0 mV, the latter estimations do not provide information about the true P_o of the channel. The application of the binomial model to few channel preparations predicted that P_o = 0.34 at V_j = 0 mV; this value should be considered as an upper bound because of the possible underestimation of the number of channels present at the junctional membrane. The shapes of the distributions of G_{ss}/G_{max} and P_o as a function of V_j are very similar at large driving forces but differ slightly at low transjunctional voltages. Several possibilities can be proposed to explain this difference, including the limited resolution of single channels at low V_j under dual whole cell patch clamp conditions. First, the presence of a second channel population might have substantially modified the junctional conductance-transjunctional voltage relationship of macroscopic data. Indeed, a smaller gap junction channel with a size of 25–28 pS was observed in 22% of the weakly coupled cell pairs. Although these cell pairs were not used for single channel kinetic analysis, the presence of this smaller channel could not be ruled out from the macroscopic data. Second, factors other than voltage may participate in the gating of the channels which might explain the heterogenity of junctional conductances that was observed among Schwann cell pairs. In this context, modulation of gating properties of heart-type gap junction channels by differential phosphorylation of Cx43 has been reported (Moreno, Fishman, and Spray, 1992). Third, additional voltage dependent shut states of the channels could

not be completely ruled out in our experiments. This possibility is however unlikely because rapid closures comprising bursts during channel opening were not observed (if present but undetectable due to data filtering, the residence times in such states would be <0.025 that of the open time at low voltage).

The gap junction channel spans membranes of two cells, and this configuration allows the possibility for symmetrical gating domains contributed by each cell's hemichannel (Harris et al., 1981; Spray et al., 1981). For the Schwann cell gap junction, voltage gating for potentials of either polarity is symmetric about the 0 mV transjunctional voltage axis and relaxation kinetics are first order with identical rate constants for potentials of either polarity. Thus, the envisioned reaction scheme involves two gates in series, closing the channel from a single open state (O) to two independent closed states (C_1 and C_2; Harris et al., 1981):

$$C_1 \underset{\beta}{\overset{\alpha}{\rightleftharpoons}} O \underset{\beta}{\overset{\alpha}{\leftrightharpoons}} C_2 \tag{6}$$

When closed to state C_1 by a voltage of one polarity, this scheme predicts that the channel must first open (with time course dictated by the rate constants α and β at 0 mV) before being closed by a voltage of opposite polarity to state C_2 (where α and β are determined by the magnitude of this voltage pulse). The experiment presented in Fig. 10 of this paper demonstrates such a predicted delay in channel closing, and the recordings from low conductance pairs have allowed the underlying channel openings to be visualized. To date, it remains uncertain whether each gate on the gap junction channel is regulated contingently or independently. Indeed, while the former model did fit the I_j behavior of Cx38 expressed by *Xenopus* embryos (Harris et al., 1981) and Cx32 introduced in a communication-deficient cell line (Moreno et al., 1991*b*), independent gating was favored to explain experiments performed on neonatal hamster myocytes (Wang et al., 1992).

In conclusion, macroscopic and single channel approaches used here to analyze the kinetics of Schwann cell gap junctional currents led to the same qualitative conclusion; i.e., that voltage-dependent gating of the channels can be described by a two-state model. However, because of resolution limits imposed by the experimental conditions, the possibility of a more complex gating behavior of the channels cannot be totally excluded.

We thank Drs. T.A. Bargiello, A.P. Moreno, J. Rubin, and V.K. Verselis for comments and support during the preparation of this work.

Supported in part by NIH grants NS 16524 to D.C. Spray and NS 07512 to M. V. L. Bennett (subprojects to D. C. Spray and J. A. Kessler). M. Chanson is a Fellow of the Swiss National Science Foundation; M. B. Rook was a Participating Laboratory Fellow of the New York Chapter of the American Heart Association.

Original version received 6 March 1993 and accepted version received 26 July 1993.

REFERENCES

Anumonwo, J. M. B., H.-Z. Wang, E. Trabka-Janik, B. Dunham, R. D. Veenstra, M. Delmar, and J. Jalife. 1992. Gap junctional channels in adult mammalian sinus nodal cells. *Circulation Research.* 71:229–239.

Barrio, L. C., T. Suchyna, T. A. Bargiello, L. X. Xu, R. S. Roginsky, M. V. L. Bennett, and B. J. Nicholson. 1991. Gap junctions formed by connexins 26 and 32 alone and in combination are differently affected by applied voltage. Proceedings of the National *Academy of Sciences USA.* 88:8410–8414.

Bennett, M. V. L., and D. C. Spray, editors. 1985. Gap Junctions. Cold Spring Harbor Laboratories, Cold Spring Harbor, New York. 409 pp.

Beyer, E. C., D. L. Paul, and D. A. Goodenough. 1990. Connexin family of gap junction proteins. *Journal of Membrane Biology.* 116:187–194.

Brockes, J. P., K. L. Fields, and M. C. Raff. 1979. Studies on cultured rat Schwann cells. I. Establishment of purified populations from cultures of peripheral nerve. *Brain Research.* 165:105–118.

Chandross, K., M. Chanson, D. C. Spray, and J. A. Kessler. 1992. Growth factor induced phenotypic changes in cultured Schwann cells include altered gap junctional conductance. *Society for Neuroscience Abstracts.* 18:960*a*. (Abstr.)

Colquhoun, D., and A. G. Hawkes. 1983. The principles of the stochastic interpretation of ion-channel mechanisms. *In* Single Channel Recording. B. Sakmann, and E. Neher, editors. Plenum Publishing Corp., New York. 135–177.

Dahl, G., T. Miller, D. Paul, R. Voellmy, and R. Werner. 1987. Expression of functional cell–cell channels from cloned rat liver gap junction complementary DNA. *Science.* 236:1290–1293.

Dermietzel, R., T. K. Hwang, and D. C. Spray. 1990. The gap junction family: structure, function and chemistry. *Anatomy and Embryology.* 182:517–528.

Eghbali, B., J. A. Kessler, and D. C. Spray. 1990. Expression of gap junction channels in a communication incompetent cell line after transfection with connexin32 cDNA. *Proceedings of the National Academy of Sciences, USA.* 87:1328–1331.

Fishman, G. I., R. L. Eddy, T. B. Shows, L. Rosenthal, and L. A. Leinwand. 1991*a*. The human connexin gene family of gap junction proteins: distinct chromosomal locations but similar structures. *Genomics.* 10:250–256.

Fishman, G. I., A. P. Moreno, D. C. Spray, and L. A. Leinwand. 1991*b*. Functional analysis of human cardiac gap junction channel mutants. *Proceedings of the National Academy of Sciences, USA.* 88:3525–3529.

Giaume, C., C. Fromaget, A. El Aoumari, J. Cordier, J. Glowinsky, and D. Gros. 1991. Gap junctions in cultured astrocytes: single-channel currents and characterization of channel-forming protein. *Neuron.* 6:133–143.

Giaume, C., R. T. Kado, and H. Korn. 1987. Voltage-clamp analysis of a crayfish rectifying synapse. *Journal of Physiology.* 386:91–112.

Haefliger, J. H., R. Bruzzone, N. A. Jenkins, D. J. Gilbert, N. G. Copeland, and D. L. Paul. 1992. Four novel members of the connexin family of gap junction proteins. Molecular cloning, expression and chromosome mapping. *Journal of Biological Chemistry.* 267:2057–2064.

Hall, J. E., G. A. Zampighi, and R. M. Davis, editors. 1993. Gap Junctions. Progress in Cell Research. Vol. 3. Elsevier Science Publishers, Amsterdam, Holland. 333 pp.

Harris, A. L., D. C. Spray, and M. V. L. Bennett. 1981. Kinetic properties of a voltage-dependent junctional conductance. *Journal of General Physiology.* 77:95–117.

Hertzberg, E. L., and R. G. Johnson, editors. 1988. Gap Junctions. Modern Cell Biology Vol. 7. Alan R. Liss, Inc., New York. 548 pp.

Lal, R., and M. F. Arnsdorf. 1992. Voltage dependent gating and single-channel conductance of adult mammalian atrial gap junctions. *Circulation Research.* 71:737–743.

Loewenstein, W. R. 1979. Junctional intercellular communication and the control of growth. *Biochemica et Biophysica Acta.* 560:1–65.

Manivannan, K., S. V. Ramanan, R. T. Mathias, and P. R. Brink. 1992. Multichannel recordings from membranes which contain gap junctions. *Biophysical Journal.* 61:216–226.

Meda, P., D. Bosco, E. Giordano, and M. Chanson. 1991. Junctional coupling modulation by secretagogues in two-cell pancreatic systems. *In* Biophysics of Gap Junction Channels. C. Peracchia, editor, CRC Press Inc., Boca Raton, FL. 191–208.

Moreno, A. P., A. C. Campos de Carvalho, G. J. Christ, A. Melman, and D. C. Spray. 1993. Gap junctions between human *corpus cavernosum* smooth muscle cells: gating properties and unitary conductance. *American Journal of Physiology.* 264:C80–C92.

Moreno, A. P., A. C. Campos de Carvalho, V. K. Verselis, B. Eghbali, and D. C. Spray. 1991*a*. Voltage-dependent gap junction channels are formed by connexin32, the major gap junction protein of rat liver. *Biophysical Journal.* 59:920–925.

Moreno, A. P., B. Eghbali, and D. C. Spray. 1991*b*. Equilibrium and steady-state properties of connexin32 gap junction channels, as revealed in stably transfected cells. *Biophysical Journal.* 60:1267–1277.

Moreno, A. P., G. I. Fishman, and D. C. Spray. 1992. Phosphorylation shifts unitary conductance and modifies voltage dependent kinetics of human connexin43 gap junction channels. *Biophysical Journal.* 62:51–53.

Neyton, J., and A. Trautmann. 1985. Single-channel currents of an intercellular junction. *Nature.* 317:331–335.

Porter, B., M. B. Clark, L. Glaser, and R. P. Bunge. 1986. Schwann cells stimulated to proliferate in the absence of neurons retain full functional capability. *The Journal of Neuroscience.* 6:3070–3078.

Rook, M. B., H. J. Jongsma, and A. C. G. Van Ginneken. 1988. Properties of single gap junctional channels between isolated neonatal rat heart cells. *American Journal of Physiology.* 255:H770–H782.

Rook, M. B., A. C. G. van Ginneken, B. de Jonge, A. El Aoumari, D. Gros, and H. J. Jongsma. 1992. Differences in gap junction channels between cardiac myocytes, fibroblasts and heterologous pairs. *American Journal of Physiology.* 263:C959–C977.

Rubin, J. B., V. K. Verselis, M. V. L. Bennett, and T. A. Bargiello. 1992. A domain substitution procedure and its use to analyze voltage dependence of gap junctions formed by connexins 26 and 32. *Proceedings of the National Academy of Sciences, USA.* 89:3820–3824.

Rüdisüli, A., and R. Weingart. 1989. Electrical properties of gap junction channels in guinea-pig ventricular cell pairs revealed by exposure to heptanol. *Pfluegers Archives.* 415:12–21.

Spray, D. C., and J. M. Burt. 1990. Structure-activity relations of the cardiac gap junction channel. *American Journal of Physiology.* 258:C195–C205.

Spray, D. C., A. L. Harris, and M. V. L. Bennett. 1981. Equilibrium properties of a voltage-dependent junctional conductance. *Journal of General Physiology.* 77:77–93.

Spray, D. C., R. L. White, V. K. Verselis, and M. V. L. Bennett. 1985. General and comparative physiology of gap junction channels. *In* Gap Junctions. M. V. L. Bennett and D. C. Spray, editors. Cold Spring Harbor Laboratories, Cold Spring Harbor, NY. 139–153.

Veenstra, R. D. 1990. Voltage-dependent gating of gap junction channels in embryonic chick ventricular cell pairs. *American Journal of Physiology.* 258:C662–C672.

Veenstra, R. D., and R. L. De Haan. 1986. Measurement of single channel currents from cardiac gap junctions. *Science.* 233:972–974.

Veenstra, R. D., H.-Z. Wang, E. M. Westphale, and E. C. Beyer. 1992. Multiple connexins confer distinct regulatory and conductance properties of gap junctions in developing heart. *Circulation Research.* 71:1277–1283.

Verselis, V. K., M. V. L. Bennett, and T. A. Bargiello. 1991. A voltage-dependent gap junction channel in *Drosophila melanogaster*. *Biophysical Journal.* 59:114–126.

Wang, H.-Z., J. Li, L. F. Lemanski, and R. D. Veenstra. 1992. Gating of mammalian cardiac gap junction channels by transjunctional voltage. *Biophysical Journal.* 63:139–151.

Warner, A. E., S. C. Guthrie, and N. B. Gilula. 1984. Antibodies to gap junctional protein selectively disrupt junctional communication in the early amphibian embryo. *Nature.* 311:127–131.

White, T. W., R. Bruzzone, D. A. Goodenough, and D. L. Paul. 1992. Mouse Cx50, a functional member of the connexin family of gap junction proteins, is the lens fiber protein MP70. *Molecular Biology of the Cell.* 3:711–720.

White, R. L., D. C. Spray, A. C. Campos de Carvalho, B. A. Wittenberg, and M. V. L. Bennett. 1985. Some electrical and pharmacological properties of gap junctions between adult ventricular myocytes. *American Journal of Physiology.* 249:C447–C455.

Willecke, K., R. Heynkes, E. Dahl, R. Stutenkemper, H. Hennemann, S. Jungbluth, T. Suchyna, and B. Nicholson. 1991. Mouse connexin37: cloning and functional expression of a gap junction gene highly expressed in lung. *Journal of Cell Biology.* 114:1049–1057.